Interferon Resistance of Emerging SARS-CoV-2 Variants

Kejun Guo[1], Bradley S. Barrett[1], Kaylee L. Mickens[1,2], Kim J. Hasenkrug[3]
and Mario L. Santiago[1,2]*

[1]*Division of Infectious Diseases, Department of Medicine,*
University of Colorado Anschutz Medical Campus, Aurora, CO, USA 80045

[2]*Department of Immunology and Microbiology,*
University of Colorado Anschutz Medical Campus, Aurora, CO, USA 80045

[3]*Rocky Mountain Laboratories, National Institutes of Allergy and Infectious Diseases,*
National Institutes of Health, Hamilton, MT 59840

*To whom correspondence should be addressed: mario.santiago@ucdenver.edu

The emergence of SARS-CoV-2 variants with enhanced transmissibility, pathogenesis and resistance to vaccines presents urgent challenges for curbing the COVID-19 pandemic. While Spike mutations that enhance virus infectivity may drive the emergence of these novel variants, studies documenting a critical a role for interferon responses in the early control of SARS-CoV-2 infection, combined with the presence of viral genes that limit these responses, suggest that interferons may also influence SARS-CoV-2 evolution. Here, we compared the potency of 17 different human interferons against 5 viral lineages sampled during the course of the global outbreak that included ancestral and emerging variants. Our data revealed increased interferon resistance in emerging SARS-CoV-2 variants, indicating that evasion of innate immunity is a significant driving force for SARS-CoV-2 evolution. These findings have implications for the increased lethality of emerging variants and highlight the interferon subtypes that may be most successful in the treatment of early infections.

The human genome encodes a diverse array of antiviral interferons (IFNs). These include the type I IFNs (IFN-Is) such as the 12 IFNα subtypes, IFNβ and IFNω that signal through ubiquitous IFNAR receptor, and the type III IFNs (IFN-IIIs) such as IFNλ1, IFNλ2 and IFNλ3 that signal through the more restricted IFNλR receptor that is present in lung epithelial cells[1]. IFN diversity may be driven by an evolutionary arms-race to enable the host to counteract diverse viral pathogens[2]. For instance, the IFNα subtypes exhibit >78% amino acid sequence identity, but IFNα14, IFNα8 and IFNα6 most potently inhibited HIV-1 *in vitro* and *in vivo*[3-5], whereas IFNα5 most potently inhibited influenza H3N2 in lung explant cultures[6]. Surprisingly, while SARS-CoV-2 was sensitive to IFNα2, IFNβ, and IFNλ[7-9], and clinical trials on IFNα2 and IFNβ demonstrated

43 promising outcomes against COVID-19[10-12], a direct comparison of multiple IFN-Is and IFN-IIIs
44 against diverse SARS-CoV-2 isolates has not yet been undertaken.
45

46 **Results**

47 The current study was undertaken to determine which IFNs would best inhibit SARS-CoV-2. We
48 selected 5 isolates from prominent lineages[13] during the course of the pandemic (Fig. 1,
49 Supplementary Table 1). USA-WA1/2020 is the standard strain utilized in many *in vitro* and *in*
50 *vivo* studies of SARS-CoV-2 and belongs to lineage A[13]. It was isolated from the first COVID-19
51 patient in the US, who had a direct epidemiologic link to Wuhan, China, where the virus was first
52 detected[14]. By contrast, subsequent infection waves from Asia to Europe[15] were associated with
53 the emergence of the D614G mutation[16]. D614G+ strains in lineage B spread with devastating
54 speed, likely due to its increased transmissibility[17,18]. It accumulated additional mutations in Italy
55 as lineage B.1 which then precipitated a severe outbreak in New York City[19]. More recently,
56 lineage B.1.1.7 acquired the N501Y mutation that is associated with enhanced transmissibility in
57 the United Kingdom[13]. Lineage B.1.351 was first reported in South Africa and acquired an
58 additional E484K mutation that is associated with resistance to neutralizing antibodies[20,21]. Both
59 B.1.1.7 and B.1.351 have now been reported in multiple countries and there is increasing concern
60 that these may become dominant[22]. Representative SARS-CoV-2 isolates from the B, B.1, B.1.1.7
61 and B.1.351 lineages were obtained from BEI Resources (Supplementary Table 1) and amplified
62 once in an alveolar type II epithelial cell line, A549, that we stably transduced with the receptor
63 ACE2 (A549-ACE2) (Supplementary Fig. 1a).
64

65 A549-ACE2 cells were pre-incubated with 17 recombinant IFNs (PBL Assay Science) overnight
66 in parallel and in triplicate, then infected with a non-saturating virus dose for 2 h (Supplementary
67 Fig. 1b). We normalized the IFNs based on molar concentrations similar to our previous work with
68 HIV-1[3,23]. For rapid and robust evaluation of antiviral activities against live SARS-CoV-2 isolates,
69 we utilized a quantitative PCR approach (Fig. 2a). An initial dose-titration study showed that a 2
70 pM concentration maximally distinguished the antiviral activities of IFNβ and IFNλ1
71 (Supplementary Fig. 1c), and was therefore used to screen the antiviral IFNs. In the absence of
72 IFN, all 5 isolates reached titers of ~10^4-10^6 copies per 5 µl input of RNA extract (Fig. 2). Using
73 absolute copy numbers (Fig. 2) and values normalized to mock as 100% (Supplementary Fig. 2),
74 the 17 IFNs showed a range of antiviral activities against SARS-CoV-2. The 3 IFNλ subtypes
75 exhibited none to very weak (<2-fold) antiviral activities compared to most IFN-Is (Fig. 2 and
76 Supplementary Fig. 2, blue bars). This was despite the fact that the assay showed a robust dynamic
77 range, with some IFNs inhibiting USA-WA1/2020 >2500-fold to below detectable levels (Fig. 2a).
78 IFN potencies against the 5 isolates correlated with each other (Supplementary Fig. 3), and a
79 similar rank-order of IFN antiviral potency was observed for D614G+ isolates (Fig. 2b,
80 Supplementary Fig. 2). Overall, IFNα8, IFNβ and IFNω were the most potent, followed by IFNα5,
81 IFNα17 and IFNα14 (Fig. 2c).
82
83 We reported that HIV-1 inhibition by the IFNα subtypes correlated with IFNAR signaling capacity
84 and binding affinity to the IFNAR2 subunit[3,23]. IFNAR signaling capacity, as measured in an IFN-
85 sensitive reporter cell line (iLite cells; Euro Diagnostics), correlated with the antiviral potencies of
86 the IFNα subtypes against SARS-CoV-2 lineages A and B, but not B.1, B.1.351 or B.1.1.7 strains
87 (Fig. 3a). Interestingly, IFNα subtype inhibition of SARS-CoV-2 did not correlate with IFNAR2

88 binding affinity (Fig. 3b)[24], as measured by surface plasmon resonance by the Schreiber group[24].
89 Furthermore, correlations between SARS-CoV-2 and HIV-1 inhibition[3] were weak at best (Fig.
90 3c). These findings suggested that IFN-mediated control of SARS-CoV-2 isolates may be
91 qualitatively distinct from that of HIV-1.
92
93 We generated a heat-map to visualize the antiviral potency of diverse IFNs against the 5 isolates
94 and observed marked differences in IFN sensitivities (Fig. 4a). Pairwise analysis of antiviral
95 potencies between isolates collected early (January 2020) and later (March-December 2020)
96 during the pandemic were performed against the 14 IFN-Is (IFN-IIIs were not included due to low
97 inhibition, Fig. 2). The overall IFN-I sensitivity of USA-WA1/2020 and Germany/BavPat1/2020
98 isolates were not significantly different from each other (Fig. 4b). By contrast, relative to
99 Germany/BavPat1/2020, we observed 17 to 122-fold IFN-I resistance of the emerging SARS-
100 CoV-2 variants (Fig. 4c), with the B.1.1.7 strain exhibiting the highest IFN-I resistance. The level
101 of interferon resistance was more striking when compared to USA-WA1/2020, where emerging
102 SARS-CoV-2 variants exhibited 25 to 322-fold higher IFN-I resistance (Supplementary Fig. 4a).
103
104 The experiments above allowed the simultaneous analysis of 17 IFNs against multiple SARS-
105 CoV-2 isolates, but do not provide information on how different IFN-I doses affect virus
106 replication. It also remains unclear if the emerging variants were resistant to IFN-IIIs. We therefore
107 titrated a potent (IFNβ; 0.002 to 200 pM) and a weak (IFNλ1; 0.02 to 2000 pM) interferon against
108 the lineage B, B.1, B.1.1.7 and B.1.351 isolates (Fig. 4d and Supplementary Fig. 4b). We included
109 an additional B.1.1.7 strain, hCov-19/England/204820464/2020 (Supplementary Table 1). The
110 50% inhibitory concentrations (IC_{50}) of the B.1.1.7 variants were 4.3 to 8.3-fold higher for IFNβ

111 and 3.0 to 3.5 higher for IFNλ1 than the lineage B isolate (Fig. 4d), whereas the B.1 isolate
112 exhibited 2.6 and 5.5-fold higher IC_{50} for IFNλ1 and IFNβ, respectively (Supplementary Fig. 4b).
113 Interestingly, maximum inhibition was not achieved with either IFNβ or IFNλ1 against the B.1.1.7
114 variant, plateauing at 15 to 20-fold higher levels than the ancestral lineage B isolate (Fig. 4d). In
115 a separate experiment, the B.1.351 variant was also more resistant to IFNβ (>500-fold) and IFNλ1
116 (26-fold) compared to the lineage B isolate (Fig. 4d). These data confirm that the B.1, B.1.1.7 and
117 B.1.351 isolates have evolved to resist the IFN-I and IFN-III response.
118

119 **Discussion**

120 Numerous studies done by many laboratories highlighted the importance of IFNs in SARS-CoV-
121 2 control. Here, we demonstrate the continued evolution of SARS-CoV-2 to escape IFN responses
122 and identify the IFNs with the highest antiviral potencies. IFNλ initially showed promise as an
123 antiviral that can reduce inflammation[25], but was recently associated with virus-induced lung
124 pathology[26]. Our data suggests that higher doses of IFNλ may be needed to achieve a similar
125 antiviral effect *in vivo* as the IFN-Is. Nebulized IFNβ showed potential as a therapeutic against
126 COVID-19[11], and our data confirm IFNβ as a highly potent antiviral against SARS-CoV-2.
127 However, IFNβ was also linked to pathogenic outcomes in chronic mucosal HIV-1[23], murine
128 LCMV[27] and if administered late in mice, SARS-CoV-1 and MERS-CoV[28,29] infection. By
129 contrast, IFNα8 altered 3-fold less genes in primary mucosal lymphocytes than IFNβ[23], but showed
130 similar anti-SARS-CoV-2 potency as IFNβ. IFNα8 also exhibited high antiviral activity against
131 HIV-1[3], raising its potential for treatment against both pandemic viruses. Notably, IFNα8 appeared
132 to be an outlier, as the antiviral potencies of the IFNα subtypes against SARS-CoV-2 and HIV-1
133 did not strongly correlate. IFNα6 potently restricted HIV-1[3,4] but was one of the weakest IFNα

134 subtypes against SARS-CoV-2. Conversely, IFNα5 strongly inhibited SARS-CoV-2, but weakly
135 inhibited HIV-1[3]. Our data strengthens the theory that diverse IFNs may have evolved to restrict
136 distinct virus families[2,23]. The mechanisms underlying these qualitative differences remain unclear.
137 While IFNAR signaling contributes to antiviral potency[3,4,24], diverse IFNs may have distinct
138 abilities to mobilize antiviral effectors in specific cell types. Comparing the interferomes induced
139 by distinct IFNs in lung epithelial cells may help unravel antiviral mechanisms that is responsible
140 for the differential effects.
141
142 Our data unmasked a concerning trend for emerging SARS-CoV-2 variants to resist the antiviral
143 IFN response. Prior to this work, the emergence and fixation of variants was linked to enhanced
144 viral infectivity due to mutations in the Spike protein[13,16-18]. However, previous studies on HIV-1
145 infection suggested that IFNs can also shape the evolution of pandemic viruses[30,31]. In fact, SARS-
146 CoV-2 infected individuals with either genetic defects in IFN signaling[32] or IFN-reactive
147 autoantibodies[33] had increased risk of developing severe COVID-19. As IFNs are critical in
148 controlling early virus infection levels, IFN-resistant SARS-CoV-2 variants may produce higher
149 viral loads that could in turn promote transmission and/or exacerbate pathogenesis. Consistent with
150 this hypothesis, alarming preliminary reports linked B.1.1.7 with increased viral loads[34] and risk
151 of death[35-37]. In addition to Spike, emerging variants exhibited mutations in nucleocapsid,
152 membrane and nonstructural proteins NSP3, NSP6 and NSP12 (Supplementary Table 1). These
153 viral proteins were shown to antagonize IFN signaling in cells[38-40]. It will be important to identify
154 the virus mutations driving IFN-I resistance in emerging variants, the underlying molecular
155 mechanisms, and its consequences for COVID-19 pathogenesis.
156

157 Overall, the current study suggested a role for the innate immune response in driving the evolution
158 of SARS-CoV-2 that could have practical implications for interferon-based therapies. Our findings
159 reinforce the importance of continued full-genome surveillance of SARS-CoV-2, and assessments
160 of emerging variants not only for resistance to vaccine-elicited neutralizing antibodies, but also for
161 evasion of the host interferon response.
162

163 ## Materials and Methods
164
165 **Cell lines.** A549 cells were obtained from the American Type Culture Collection (ATCC) and
166 cultured in complete media containing F-12 Ham's media (Corning), 10% fetal bovine serum
167 (Atlanta Biologicals), 1% penicillin/streptomycin/glutamine (Corning) and maintained at 37°C 5%
168 CO_2. A549 cells were transduced with codon-optimized human ACE2 (Genscript) cloned into
169 pBABE-puro[41] (Addgene). To generate the A549-ACE2 stable cell line, 10^7 HEK293T (ATCC)
170 cells in T-175 flasks were transiently co-transfected with 60 µg mixture of pBABE-puro-ACE2,
171 pUMVC, and pCMV-VSV-G at a 10:9:1 ratio using a calcium phosphate method[42]. Forty-eight
172 hours post transfection, the supernatant was collected, centrifuged at 1000×*g* for 5 min and passed
173 through a 0.45 µm syringe filter to remove cell debris. The filtered virus was mixed with fresh
174 media (30% vol/vol) that included polybrene (Sigma) at a 6 µg/ml final concentration. The virus
175 mixture was added into 6-well plates with 5×10^5 A549 cells/well and media was changed once
176 more after 12 h. Transduced cells were selected in 0.5 µg/ml puromycin for 72 h, and ACE2
177 expression was confirmed by flow cytometry, western blot and susceptibility to HIV-
178 1ΔEnv/SARS-CoV-2 Spike pseudovirions.
179

180 **Virus isolates.** All experiments with live SARS-CoV-2 were performed in a Biosafety Level-3
181 (BSL3) facility with powered air-purifying respirators at the University of Colorado Anschutz
182 Medical Campus. SARS-CoV-2 stocks from BEI Resources (Supplementary Table 1) had
183 comparable titers $>10^6$ $TCID_{50}$/ml (Supplementary Fig. 1a) except for the B.1.1.7 strains
184 (CA_CDC_5574/2020 and England/204820464/2020). The contents of the entire vial (~0.5 ml)
185 were inoculated into 3 T-75 flasks containing 3×10^6 A549-ACE2 cells, except for B.1.1.7 which
186 was inoculated into 1 T-75 flask. After culturing for 72 h, the supernatants were collected and spun
187 at 2700×*g* for 5 min to remove cell debris, and frozen at -80°C. The A549-amplified stocks were
188 titered according to the proposed assay format (Supplementary Fig. 1b, Fig. 2a). Briefly, 2.5×10^4
189 A549-ACE2 cells were plated per well in a 48-well plate overnight. The next day, the cells were
190 infected with 300, 30, 3, 0.3, 0.03 and 0.003 µl (serial 10-fold dilution) of amplified virus stock in
191 300 µl final volume of media for 2 h. The virus was washed twice with PBS, and 500 µl of
192 complete media with the corresponding IFN concentrations were added. After 24 h, supernatants
193 were collected, and cell debris was removed by centrifugation at 3200×*g* for 5 min.
194
195 **SARS-CoV-2 quantitative PCR.** For rapid and robust assessments of viral replication, we utilized
196 a real-time quantitative PCR (qPCR) approach. This assay would require less handling of
197 infectious, potentially high-titer SARS-CoV-2 in the BSL3 compared to a VeroE6 plaque assay,
198 as the supernatants can be directly placed in lysis buffer containing guanidinium thiocyanate that
199 would inactivate the virus by at least 4-5 $\log_{10}$[43]. To measure SARS-CoV-2 levels, total RNA was
200 extracted from 100 µl of culture supernatant using the E.Z.N.A Total RNA Kit I (Omega Bio-Tek)
201 and eluted in 50 µl of RNAse-free water. 5 µl of this extract was used for qPCR. Official CDC

202 SARS-CoV-2 N1 primers and TaqMan probe set were used[44] with the Luna Universal Probe One-
203 Step RT-qPCR Kit (New England Biolabs):

204 Forward primer: `GACCCCAAAATCAGCGAAAT`

205 Reverse primer: `TCTGGTTACTGCCAGTTGAATCTG`

206 TaqMan probe: `FAM-ACCCCGCATTACGTTTGGTGGACC-TAMRA`

207 The sequence of the primers and probes were conserved against the 5 SARS-CoV-2 variants that
208 were investigated. The real-time qPCR reaction was run on a Bio-Rad CFX96 real-time
209 thermocycler under the following conditions: 55°C 10 mins for reverse transcription, then 95°C 1
210 min followed by 40 cycles of 95°C 10s and 60°C 30s. The absolute quantification of the N1 copy
211 number was interpolated using a standard curve with 10^7-10^1 serial 10-fold dilution of a control
212 plasmid (nCoV-CDC-Control Plasmid, Eurofins).

213

214 **Antiviral inhibition assay.** We used a non-saturating dose of the amplified virus stock for the IFN
215 inhibition assays. These titers were expected to yield ~10^5 copies per 5 µl input RNA extract
216 (Supplementary Fig. 1b). Recombinant IFNs were obtained from PBL Assay Science. In addition
217 to the IFN-Is (12 IFNα subtypes, IFNβ and IFNω), we also evaluated 3 IFNλ subtypes (IFNλ1,
218 IFNλ2, IFNλ3). To normalize the IFNs, we used molar concentrations[23] instead of international
219 units (IU), as IU values were derived from inhibition of encelphalomyocarditis virus, which may
220 not be relevant to SARS-CoV-2. To find a suitable dose to screen 17 IFNs in parallel, we
221 performed a dose-titration experiment of the USA-WA1/2020 strain with IFNβ and IFNλ1. A dose
222 of 2 pM allowed for maximum discrimination of the antiviral potency IFNβ versus IFNλ1
223 (Supplementary Fig. 1c). Serial 10-fold dilutions of IFNβ and IFNλ1 were also used in follow-up
224 experiments. Thus, in 48-well plates, we pre-incubated 2.5×10^4 A549-ACE2 cells with the IFNs

225 for 18 h, then infected with the A549-amplified virus stock for 2 h. After two washes with PBS,
226 500 µl complete media containing the corresponding IFNs were added. The cultures were
227 incubated for another 24 h, after which, supernatants were harvested for RNA extraction and qPCR
228 analysis.
229
230 **Statistical analyses.** Data were analyzed using GraphPad Prism 8. Differences between the IFNs
231 were tested using a nonparametric two-way analysis of variance (ANOVA) followed by a multiple
232 comparison using the Friedman test. Pearson correlation coefficients (R^2) values were computed
233 for linear regression analyses. Paired analysis of two isolates against multiple IFNs were
234 performed using a nonparametric, two-tailed Wilcoxon matched-pairs rank test. Differences with
235 $p<0.05$ were considered significant. Nonlinear regression curves were fit using a two-phase
236 exponential decay equation on log-transformed data.
237

238 ## Acknowledgments

239 We thank Cara Wilson, Ulf Dittmer and Kathrin Gibbert for scientific advice; Mercedes Rincon
240 and Elan Eisenmesser for assistance with construction and characterization of the A549-ACE2
241 cells; Eric Poeschla, James Morrison, Zach Wilson, Jill Garvey, Stephanie Torres-Nemeti and
242 Marcia Finucane for Biosafety Level-3 infrastructure support; and Roman Wölfel, Rosina
243 Ehmann, Adolfo García-Sastre, Alex Sigal, Tulio de Oliveira, Bassam Hallis, the CDC and BEI
244 Resources (NIAID) for the SARS-CoV-2 isolates. This work was supported by the Department of
245 Medicine at the University of Colorado (MLS), NIH R01 AI134220 (MLS), and the Intramural
246 Research Program at the NIH, NIAID (KJH).
247

248 **Figures**

249

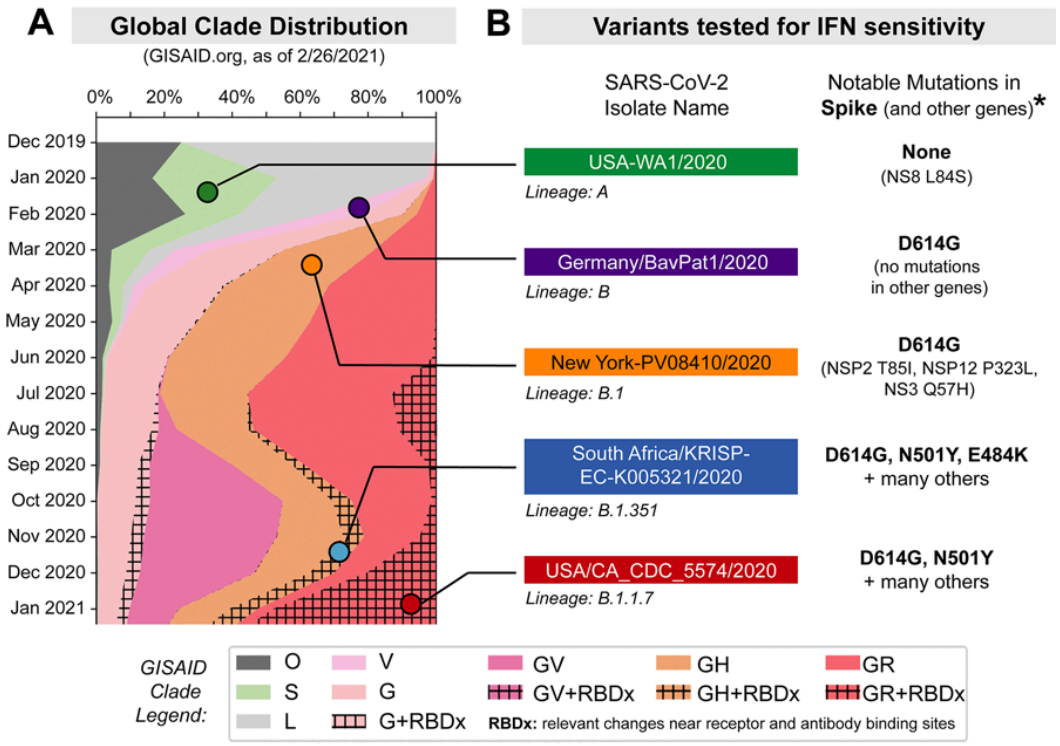

250

251

252 **Figure 1 | Selection of SARS-CoV-2 strains for IFN sensitivity studies.** (**a**) Global distribution
253 of SARS-CoV-2 clades. GISAID.org plotted the proportion of deposited sequences in designated
254 clades against collection dates. The five isolates chosen are noted by colored dots. (**b**) SARS-CoV-
255 2 strains selected for this study included representatives of lineages A, B, B.1, B.1.351 and B.1.1.7
256 (Supplementary Table 1). Lineage B isolates encode the D614G mutation associated with
257 increased transmissibility. *Amino acid mutations were relative to the reference hCOV-
258 19/Wuhan/WIV04/2019 sequence.

259

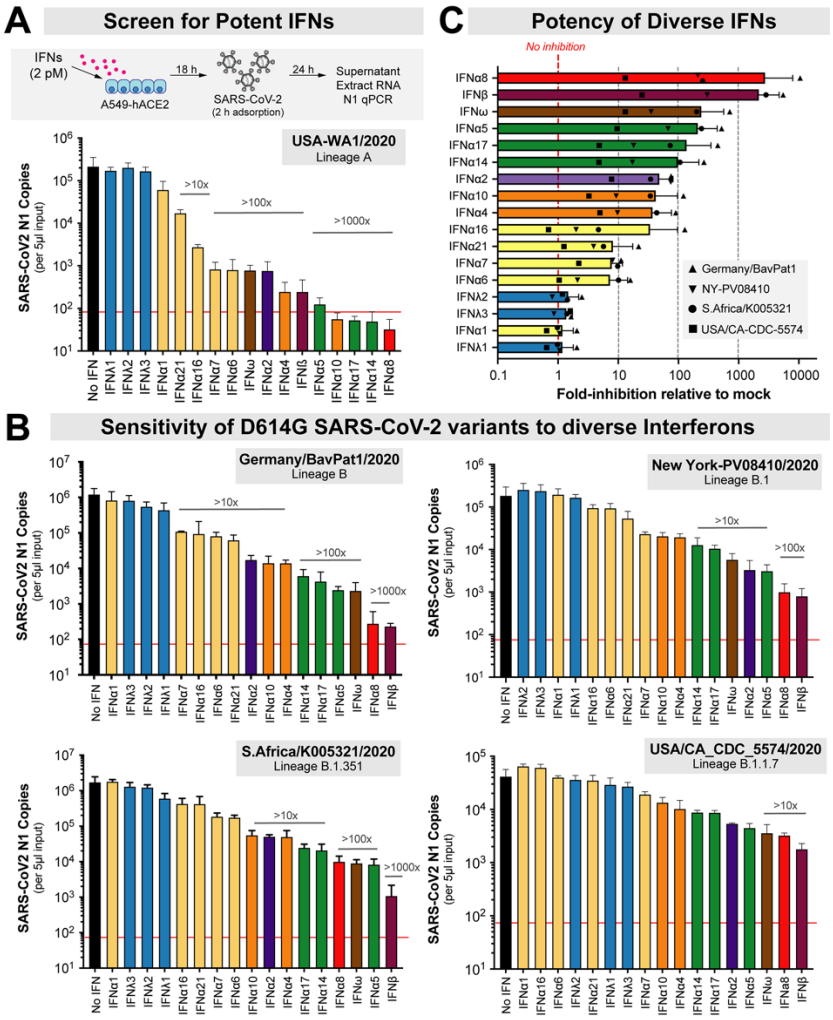

Figure 2 | Sensitivity of SARS-CoV-2 strains to IFN-I and IFN-III interferons. (**a**) Antiviral assay using recombinant IFNs (2 pM) in A549-ACE2 cells. The red line corresponds to the qPCR detection limit (<90 copies/reaction). (**b**) Viral copy numbers in D614G+ isolates, showing a similar rank-order of IFNs from least to most potent. (**c**) The average fold-inhibition relative to mock for lineage B, B.1, B.1.351 and B.1.1.7 isolates are shown. The most potent IFNs are shown top to bottom. For all panels, bars and error bars correspond to means and standard deviations.

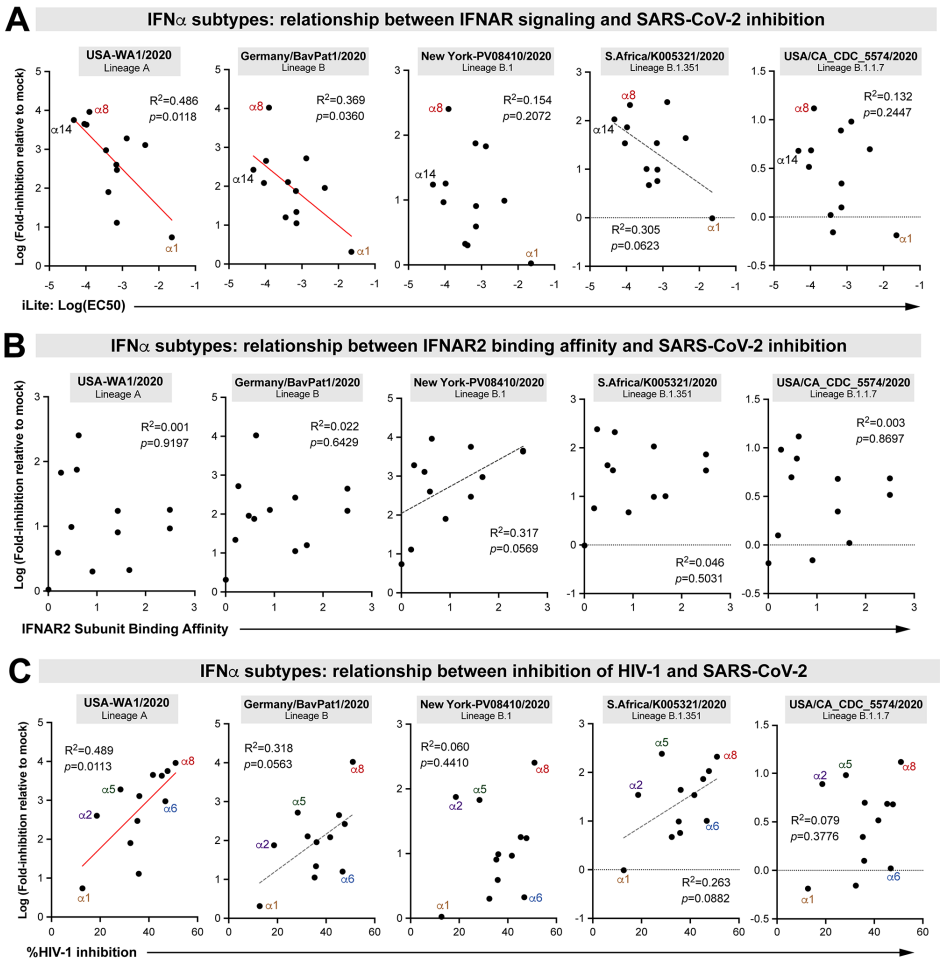

Figure 3 | Correlation between SARS-CoV-2 inhibition and biological properties of IFNα subtypes. Log-transformed IFN-inhibition values relative to mock for the 5 different SARS-CoV-2 strains were compared to previously published values on (**a**) 50% effective concentrations in the iLite assay, a reporter cell line encoding the IFN sensitive response element of *ISG15* linked to firefly luciferase[23]; (**b**) IFNAR2 subunit binding affinity, as measured by surface plasmon resonance by the Schreiber group[24]; and (**c**) HIV-1 inhibition values, based on % inhibition of HIV-1 p24+ gut lymphocytes relative to mock as measured by flow cytometry[3]. Each dot corresponds to an IFNα subtype. Linear regression was performed using GraphPad Prism 8. Significant correlations ($p<0.05$) were highlighted with a red best-fit line; those that were trending ($p<0.1$) had a gray, dotted best-fit line.

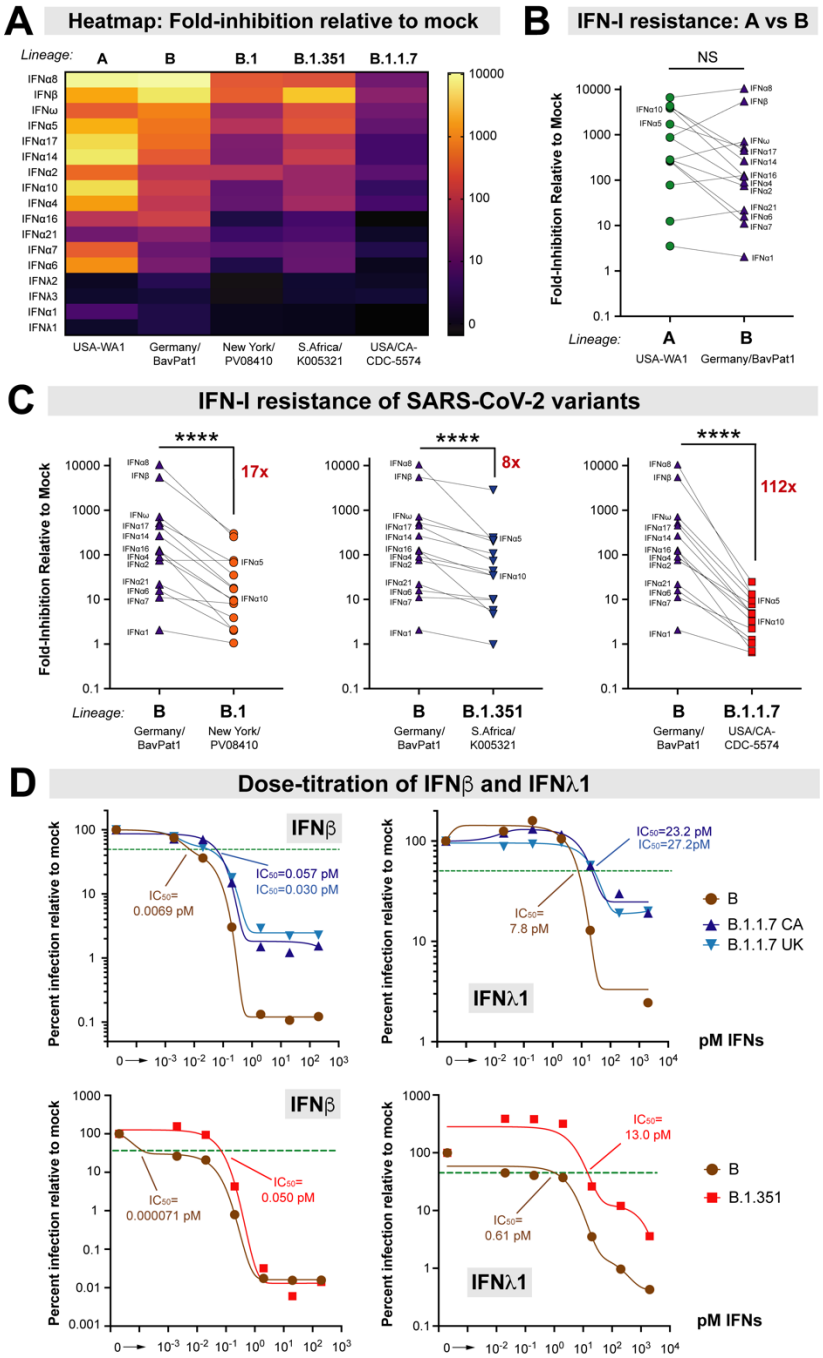

285

286 **Figure 4 | Increased interferon resistance of emerging SARS-CoV-2 variants.** (**a**) Heatmap of
287 fold-inhibition of representative strains from the lineages noted. Colors were graded on a log-scale
288 from highest inhibition (yellow) to no inhibition (black). Comparison of IFN-I sensitivities
289 between (**b**) lineage A and B isolates; and (**c**) lineage B versus B.1, B.1.351 and B.1.1.7. The mean
290 fold-inhibition values relative to mock were compared in a pairwise fashion for the 14 IFN-Is. In

291 (**c**), the average fold-inhibition values were noted. Differences were evaluated using a
292 nonparametric, two-tailed Wilcoxon matched-pairs signed rank test. NS, not significant; ****,
293 $p<0.0001$. (**d**) Dose-titration of IFNβ and IFNλ1 against lineage B (Germany/BavPat1/2020)
294 versus B.1.1.7 and B.1.351 isolates. In addition to USA/CA_CDC_5574/2020, we also evaluated
295 a second B.1.1.7 isolate from the United Kingdom (UK), England/204820464/2020. A549-ACE2
296 cells were pre-treated with serial 10-fold dilutions of IFNs for 18 h in triplicate and then infected
297 with SARS-CoV-2. Supernatants were collected after 24 h, SARS-CoV-2 N1 copy numbers were
298 determined by qPCR, and then normalized against mock as 100%. Non-linear best-fit regression
299 curves of mean normalized infection levels were used to interpolate 50% inhibitory concentrations
300 (green dotted lines).
301

302 **References**

303 1 Pestka, S., Krause, C. D. & Walter, M. R. Interferons, interferon-like cytokines, and their
304 receptors. *Immunol Rev* **202**, 8-32, doi:10.1111/j.0105-2896.2004.00204.x (2004).

305 2 Gibbert, K., Schlaak, J. F., Yang, D. & Dittmer, U. IFN-alpha subtypes: distinct biological
306 activities in anti-viral therapy. *Br J Pharmacol* **168**, 1048-1058, doi:10.1111/bph.12010
307 (2013).

308 3 Harper, M. S. *et al.* Interferon-alpha Subtypes in an Ex Vivo Model of Acute HIV-1
309 Infection: Expression, Potency and Effector Mechanisms. *PLoS Pathog* **11**, e1005254,
310 doi:10.1371/journal.ppat.1005254 (2015).

311 4 Schlaepfer, E. *et al.* Dose-Dependent Differences in HIV Inhibition by Different Interferon
312 Alpha Subtypes While Having Overall Similar Biologic Effects. *mSphere* **4**,
313 doi:10.1128/mSphere.00637-18 (2019).

314 5 Lavender, K. J. *et al.* Interferon Alpha Subtype-Specific Suppression of HIV-1 Infection
315 In Vivo. *J Virol* **90**, 6001-6013, doi:10.1128/JVI.00451-16 (2016).

316 6 Matos, A. D. R. *et al.* Antiviral potential of human IFN-alpha subtypes against influenza
317 A H3N2 infection in human lung explants reveals subtype-specific activities. *Emerg*
318 *Microbes Infect* **8**, 1763-1776, doi:10.1080/22221751.2019.1698271 (2019).

319 7 Vanderheiden, A. *et al.* Type I and Type III Interferons Restrict SARS-CoV-2 Infection of
320 Human Airway Epithelial Cultures. *J Virol* **94**, doi:10.1128/JVI.00985-20 (2020).

321 8 Felgenhauer, U. *et al.* Inhibition of SARS-CoV-2 by type I and type III interferons. *The J*
322 *Biol Chem* **295**, 13958-13964, doi:10.1074/jbc.AC120.013788 (2020).

323 9 Nchioua, R. *et al.* SARS-CoV-2 Is Restricted by Zinc Finger Antiviral Protein despite
324 Preadaptation to the Low-CpG Environment in Humans. *mBio* **11**,
325 doi:10.1128/mBio.01930-20 (2020).

326 10 Wang, N. *et al.* Retrospective Multicenter Cohort Study Shows Early Interferon Therapy
327 Is Associated with Favorable Clinical Responses in COVID-19 Patients. *Cell host &*
328 *microbe* **28**, 455-464 e452, doi:10.1016/j.chom.2020.07.005 (2020).

329 11 Monk, P. D. *et al.* Safety and efficacy of inhaled nebulised interferon beta-1a (SNG001)
330 for treatment of SARS-CoV-2 infection: a randomised, double-blind, placebo-controlled,
331 phase 2 trial. *Lancet Respir Med*, doi:10.1016/S2213-2600(20)30511-7 (2020).

332 12 Shalhoub, S. Interferon beta-1b for COVID-19. *Lancet* **395**, 1670-1671,
333 doi:10.1016/S0140-6736(20)31101-6 (2020).

334 13 Rambaut, A. *et al.* A dynamic nomenclature proposal for SARS-CoV-2 lineages to assist
335 genomic epidemiology. *Nat Microbiol* **5**, 1403-1407, doi:10.1038/s41564-020-0770-5
336 (2020).

337 14 Zhou, P. *et al.* A pneumonia outbreak associated with a new coronavirus of probable bat
338 origin. *Nature* **579**, 270-273, doi:10.1038/s41586-020-2012-7 (2020).

339 15 Worobey, M. *et al.* The emergence of SARS-CoV-2 in Europe and North America. *Science*
340 **370**, 564-570, doi:10.1126/science.abc8169 (2020).

16 Korber, B. *et al.* Tracking Changes in SARS-CoV-2 Spike: Evidence that D614G Increases Infectivity of the COVID-19 Virus. *Cell* **182**, 812-827 e819, doi:10.1016/j.cell.2020.06.043 (2020).

17 Plante, J. A. *et al.* Spike mutation D614G alters SARS-CoV-2 fitness. *Nature*, doi:10.1038/s41586-020-2895-3 (2020).

18 Hou, Y. J. *et al.* SARS-CoV-2 D614G variant exhibits efficient replication ex vivo and transmission in vivo. *Science* **370**, 1464-1468, doi:10.1126/science.abe8499 (2020).

19 Gonzalez-Reiche, A. S. *et al.* Introductions and early spread of SARS-CoV-2 in the New York City area. *Science* **369**, 297-301, doi:10.1126/science.abc1917 (2020).

20 Wibmer, C. K. *et al.* SARS-CoV-2 501Y.V2 escapes neutralization by South African COVID-19 donor plasma. *Nature Med*, doi:10.1038/s41591-021-01285-x (2021).

21 Wang, P. *et al.* Antibody Resistance of SARS-CoV-2 Variants B.1.351 and B.1.1.7. *Nature*, doi:10.1038/s41586-021-03398-2 (2021).

22 Galloway, S. E. *et al.* Emergence of SARS-CoV-2 B.1.1.7 Lineage - United States, December 29, 2020-January 12, 2021. *MMWR Morb Mortal Wkly Rep* **70**, 95-99, doi:10.15585/mmwr.mm7003e2 (2021).

23 Guo, K. *et al.* Qualitative Differences Between the IFNalpha subtypes and IFNbeta Influence Chronic Mucosal HIV-1 Pathogenesis. *PLoS Pathog* **16**, e1008986, doi:10.1371/journal.ppat.1008986 (2020).

24 Lavoie, T. B. *et al.* Binding and activity of all human alpha interferon subtypes. *Cytokine* **56**, 282-289, doi:10.1016/j.cyto.2011.07.019 (2011).

25 Davidson, S. *et al.* IFNlambda is a potent anti-influenza therapeutic without the inflammatory side effects of IFNalpha treatment. *EMBO Mol Med* **8**, 1099-1112, doi:10.15252/emmm.201606413 (2016).

26 Broggi, A. *et al.* Type III interferons disrupt the lung epithelial barrier upon viral recognition. *Science* **369**, 706-712, doi:10.1126/science.abc3545 (2020).

27 Ng, C. T. *et al.* Blockade of interferon Beta, but not interferon alpha, signaling controls persistent viral infection. *Cell host & microbe* **17**, 653-661, doi:10.1016/j.chom.2015.04.005 (2015).

28 Channappanavar, R. *et al.* IFN-I response timing relative to virus replication determines MERS coronavirus infection outcomes. *J Clin Invest* **130**, 3625-3639, doi:10.1172/JCI126363 (2019).

29 Channappanavar, R. *et al.* Dysregulated Type I Interferon and Inflammatory Monocyte-Macrophage Responses Cause Lethal Pneumonia in SARS-CoV-Infected Mice. *Cell host & microbe* **19**, 181-193, doi:10.1016/j.chom.2016.01.007 (2016).

30 Iyer, S. S. *et al.* Resistance to type 1 interferons is a major determinant of HIV-1 transmission fitness. *Proc Natl Acad Sci USA* **114**, E590-E599, doi:10.1073/pnas.1620144114 (2017).

31 Parrish, N. F. *et al.* Phenotypic properties of transmitted founder HIV-1. *Proc Natl Acad Sci USA* **110**, 6626-6633, doi:10.1073/pnas.1304288110 (2013).

381 32 Zhang, Q. *et al.* Inborn errors of type I IFN immunity in patients with life-threatening
382 COVID-19. *Science* **370**, doi:10.1126/science.abd4570 (2020).

383 33 Bastard, P. *et al.* Autoantibodies against type I IFNs in patients with life-threatening
384 COVID-19. *Science* **370**, doi:10.1126/science.abd4585 (2020).

385 34 Kidd, M. *et al.* S-variant SARS-CoV-2 lineage B1.1.7 is associated with significantly
386 higher viral loads in samples tested by ThermoFisher TaqPath RT-qPCR. *J Inf Dis*,
387 doi:10.1093/infdis/jiab082 (2021).

388 35 Horby, P. *et al.* NERVTAG note on B.1.1.7 severity. (2021).

389 36 Davies, N. G. *et al.* Increased hazard of death in community-tested cases of SARS-CoV-2
390 Variant of Concern 202012/01. *medRxiv*, doi:10.1101/2021.02.01.21250959 (2021).

391 37 Challen, R. *et al.* Risk of mortality in patients infected with SARS-CoV-2 variant of
392 concern 202012/1: matched cohort study. *BMJ* **372**, n579, doi:10.1136/bmj.n579 (2021).

393 38 Lei, X. *et al.* Activation and evasion of type I interferon responses by SARS-CoV-2. *Nat*
394 *Commun* **11**, 3810, doi:10.1038/s41467-020-17665-9 (2020).

395 39 Xia, H. *et al.* Evasion of Type I Interferon by SARS-CoV-2. *Cell reports* **33**, 108234,
396 doi:10.1016/j.celrep.2020.108234 (2020).

397 40 Mu, J. *et al.* SARS-CoV-2 N protein antagonizes type I interferon signaling by suppressing
398 phosphorylation and nuclear translocation of STAT1 and STAT2. *Cell Discov* **6**, 65,
399 doi:10.1038/s41421-020-00208-3 (2020).

400 41 Morgenstern, J. P. & Land, H. Advanced mammalian gene transfer: high titre retroviral
401 vectors with multiple drug selection markers and a complementary helper-free packaging
402 cell line. *Nucleic acids research* **18**, 3587-3596, doi:10.1093/nar/18.12.3587 (1990).

403 42 Dillon, S. M., Guo, K., Castleman, M. J., Santiago, M. L. & Wilson, C. C. Quantifying
404 HIV-1-Mediated Gut CD4+ T Cell Death in the Lamina Propria Aggregate Culture (LPAC)
405 Model *Bio-Protocol* **10**, doi:10.21769/BioProtoc.3486 (2020).

406 43 Pastorino, B. *et al.* Evaluation of Chemical Protocols for Inactivating SARS-CoV-2
407 Infectious Samples. *Viruses* **12**, doi:10.3390/v12060624 (2020).

408 44 CDC. Research Use Only 2019-Novel Coronavirus (2019-nCoV) Real-time RT-PCR
409 Primers and Probes. https://www.cdc.gov/coronavirus/2019-ncov/lab/rt-pcr-panel-primer-
410 probes.html. (2020).

411